Photoemission study of the bulk and surface electronic structure of Bi(111)

1999 J. Phys.: Condens. Matter 11 9571

(http://iopscience.iop.org/0953-8984/11/48/314)

J. Phys.: Condens. Matter **11** (1999) 9571–9580. Printed in the UK PII: S0953-8984(99)03154-9

Photoemission study of the bulk and surface electronic structure of Bi(111)

J Thomas†, G Jezequel† and I Pollini‡

† UMR CNRS-Université 6627 PALMS, Equipe de Physique des Surfaces et Interfaces, Université de Rennes I, F 35042 Rennes, France

‡ Dipartimento di Fisica, Università degli Studi di Milano, Istituto Nazionale di Fisica della Materia (INFM), Via Celoria 16, 20133 Milano, Italy

Received 1 April 1999, in final form 30 June 1999

Abstract. Angle-resolved energy distributions for photoelectrons emitted from the Bi(111) single crystal face are presented at 16.85 eV photon energy. The variation of peak-energy positions as a function of the electron emission angle shows four main dispersing features located between the Fermi level and 5 eV. The bulk electronic structure is found in qualitative agreement with the pseudopotential calculation performed by Golin along the TMU and TQW symmetry lines of the Brillouin zone. The experimental features located at $\bar{\Gamma}$ around 0.3 and 3 eV below the Fermi level are sampled in the two-dimensional Brillouin zone along the $\bar{\Gamma}\bar{M}\bar{\Gamma}$ and $\bar{\Gamma}\bar{K}\bar{X}$ symmetry directions (dispersion about 1 eV) and are assigned to electronic surface states.

1. Introduction

Angle resolved ultraviolet photoelectron spectroscopy (ARUPS) from single crystals has been widely used for investigating bulk and surface electronic states in semiconductors and metals [1–4]. This technique is here used in order to investigate the valence band structure and surface state emission near the Fermi level on the (111) face of Bi, following earlier angle resolved studies on the surface and bulk electronic structure of this semimetal. In particular, the electronic states along the ΓT symmetry line have been mapped by normal photoemission using synchrotron radiation [5, 6]. A surface state (SS) located in the spin–orbit gap near the Fermi level was evidenced on the (111) face via temperature effects and sensitivity to contamination. Its dispersion was investigated along the $\bar{\Gamma}\bar{K}\bar{X}$ symmetry direction in the surface Brillouin zone (SBZ) using 57.5 eV photons and checked against tight binding calculations [5]. A recent study using photons of 21.2 eV and 40.8 eV, produced by a high intensity microwave gas-discharge lamp, confirmed the existence and overall dispersion of this surface state and, due to the better overall resolution, showed two sharp structures of bulk origin aside from the surface state [7]. This study was motivated by the observation of superconductivity in granular systems built from well defined Bi clusters, whose characteristics (strong size dependence of the superconducting transition temperature) could be explained by the occurrence of surface conductivity, due to a strongly increased density of states $N(E_F)$ at the cluster surface [8]. Bismuth is a semimetal with the same A7 trigonal crystal structure as the other group V semimetals, arsenic and antimony [6]. The unit cell is rhombohedral and contains two atoms. The main crystal parameters at 4.2 K are the following: $a_0 = 6.3081$ Å; $\alpha = 57^\circ 19'$ and $u = 0.234\,07$. In figure 1 the crystal structure of Bi, the three-dimensional BZ [10] and its

0953-8984/99/489571+10$30.00

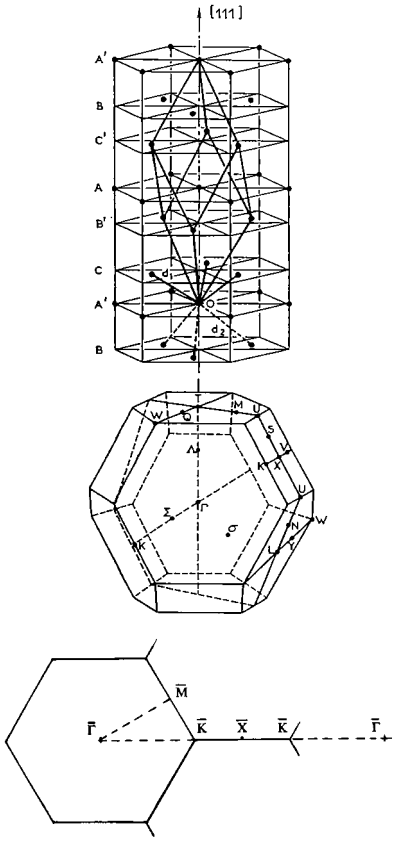

Figure 1. The bismuth crystal structure with its three-dimensional Brillouin zone and related (111) surface Brillouin zone.

related SBZ are shown. The electronic level occupation in Bi is $5d^{10}\ 6s^2\ 6p^3$ and only $6s^2$ and $6p^3$ states contribute to the occupied valence bands.

Bismuth presents interesting electronic properties, due to its small and fairly simple Fermi surface. Early investigations were carried out on amorphous, liquid and crystalline phases of Bi, where the interest was mainly to compare measured and calculated density of states (DOS) [9, 10] and to study the semimetal to metal transition of the electronic structure [11, 12]. A number of experimental studies of the Fermi surface and electronic conduction properties have been also carried out and a few band structure calculations have been accordingly made. Golin's band structure indicates that in the 0–4 eV binding energy (E_B) range three bands of p-like symmetry occur [10]. However, the electronic structure below and above the Fermi energy (E_F) is still not well known, and requires more experimental investigation; moreover, not much work has been aimed at the study and characterization of surface states in spin–orbit gaps of metals [13–15].

As a direct result of the normal photoemission study we have found that the T symmetry point is reached for the photon energy of 17 eV, as demonstrated by the photoemission peak dispersion of peaks B or C′: for example, we see in figure 5 of [6] that at $h\nu = 17$ eV the maximum (minimum) absolute binding energy is reached for the peak B (C′): such a behaviour corresponds to the point T. Thus, by using the neon I line ($h\nu = 16.8$ eV) for off normal angle

resolved photoemission, interpreted in the direct transition model and depending on the crystal azimuthal orientation, we can explore approximately the bulk electronic structure along either the TMU or TQW symmetry lines. Actually, we describe a circular arc extended in k space centred at the Γ point; that is we start from the T point in normal emission and, as we perform off normal photoemission, we deviate from these high symmetry lines slightly.

New photoemission measurements have been devised to sample the surface state bands $E(k_{\parallel})$ along the $\bar{\Gamma}\bar{K}\bar{X}$, $\bar{\Gamma}\bar{M}\bar{\Gamma}$ symmetry lines of the SBZ [16], as a non-dispersive structure of difficult interpretation was observed in normal photoemission at about 3 eV below the Fermi energy [5, 6]. Moreover, in the limit of the approximations used (direct transition model; free electron model for the final state), we have tried to map the bulk electronic structure of Bi(111) in the planes ΓLX and ΓWK, since, by starting from the T point with the right energy excitation, we actually explore, at least in the vicinity of the T point, the TMU and TQW axes, owing to the correct crystal orientation shown by Laue and low energy electron diffraction (LEED) patterns. Experimental methods are described in section 2, while photoemission results and the discussion of the electronic bulk and surface states of Bi(111) will be presented in section 3.

2. Experimental procedure

The Bi single crystal was cut at the Office National d'Etudes Aeronautiques (Chatillon-France), following the indications of the usual x-ray diagram techniques (Laue), by which we have fixed the orientation of the bulk reciprocal lattice. We have then cleaved this oriented Bi(111) crystal *in situ*, at room temperature, in order to obtain a clean and mirror-like surface from which we have performed the photoemission experiment. The crystal orientation was checked again by LEED, which confirmed the expected surface image and the choice of the symmetry lines presented in the text. In fact, by considering the LEED patterns of Bi(111), one obtains the hexagonal image of the reciprocal lattice of the SBZ normal to the $\boldsymbol{c}$ axis with threefold rotational symmetry, so that the bulk band structure is not equivalent in the two azimuths. From LEED alone we could not distinguish between the ΓM and ΓM$'$ lines in the surface zone nor between the ΓLX and Γ'L$'$X$'$ planes in the bulk BZ. However, the orientation of the bulk reciprocal lattice and surface zone was *a priori* fixed from the x-ray Laue patterns, which assured our choice of the plane of analysis and point M in the SBZ (line ΓM). The emission spectra have been measured with a monochromatized NeI resonance line (16.85 eV) as an exciting source, mainly at room temperature, except for spectra along the $\bar{\Gamma}\bar{M}\bar{\Gamma}$ line, which were measured at about 150 K. The light was incident onto the sample surface at a variable angle, while the angle between the incident photons and the electron analyser was fixed at 45° during the photoemission experiment. The energy analyser of the spectrometer has an angular acceptance of about 1.5° and an energy resolution of about 150 meV. Spectra were obtained by continuous summation of different scannings, keeping the same parameters during measurements, and the typical count rate was 2000–3000 c s^{-1}. The monochromator consists of a holographic toroidal grating with the surface covered by a gold film. Beyond the monochromator exit slit the light was focused on the sample by a toroidal mirror coated with a platinum film. The light spot on the sample was about 1 mm^2 during measurements, and the vacuum in the sample chamber, obtained by a set of ionic, cryogenic and turbomolecular pumps, was about 10^{-9} Torr. The electron detection was performed by an electrostatic hemispheric analyser (with a 48 mm bending radius and an intersphere region of 14 mm) in series with a channeltron and a frequency meter [17]. The emission polar angle was determined by rotating the sample around the cryostat axis, perpendicular both to the entrance direction of the electron analyser and to the incident beam light direction. By means of LEED the azimuthal angle φ was selected to correspond to the $\bar{\Gamma}\bar{K}\bar{X}$ (φ) and $\bar{\Gamma}\bar{M}$ ($\varphi+\pi/2$) lines of the SBZ: these high symmetry

directions correspond to the symmetry lines TW and TU in the planes ΓWK and ΓLX of the bulk Brillouin zone, respectively (see figure 1). The Fermi level energy was measured on a gold film deposited on the Bi sample, before and after the measurements. Dispersions of the bulk and surface bands have been determined by varying the polar angle θ in steps of 3° and their energy positions have been plotted as a function of the surface or bulk wavevector. These bands have been displayed along the symmetry lines in their respective BZ's, and a presentation of the experimental points is given in which surface state bands have been plotted together with bulk valence bands in the same energy diagrams.

3. Results and discussion

Figures 2 and 3 show the polar angle dependence of the ARUPS spectra measured in the ΓLX and ΓWK planes, respectively. Series of peaks and shoulders are indicated by dashes and labelled with the same letters A, A′, B, C and C′ used in normal photoemission [6] to stress the fact that the same structures have been measured along different symmetry lines. The position and intensity of the peaks are rather sensitive to the change of the polar angle and the energy dispersions of the p-like valence bands have been obtained using standard band mapping methods within the direct-transition model [1, 2]. In figures 4 and 5, we have thus plotted the energy positions of the experimental features versus the electron wavevector component $k_\parallel$ parallel to the surface, calculated by the usual formula connecting, for a given structure, the binding energy and the polar angle in the direct transition model [1, 2, 6]. In these figures, where the surface Brillouin zone is shown in the repeated zone scheme one can also follow the correspondence between the critical points of the bulk BZ and those of the SBZ illustrated in figure 1. The uncertainty of the experimental data is ± 0.1 eV for the electron energy and $\pm 1^\circ$ for the polar angle.

Let us now describe the experimental structure of the valence band of Bi, starting from high binding energy (peak C) up to the Fermi level energy. Then, we will present the surface states dispersing along the symmetry lines $\bar{\Gamma}\bar{M}\bar{\Gamma}$ and $\bar{\Gamma}\bar{K}\bar{X}$ of the SBZ, together with the bulk valence band structures (peaks C′ and B), observed along the TMU and TQW lines of the BZ and discussed in relation to Golin's band structure calculation (see figure 2 of [10]). In figures 2 and 4, we consider the region where the peaks C and C′ disperse between 3 and 4 eV. This energy region was also studied in angle resolved normal photoemission by Jezequel *et al* [5] (250 meV resolution at 20 K) and in off normal photoemission for one position of the plane of analysis (for $h\nu = 57.5$ eV). Then, Patthey *et al* [7] (40 meV resolution at 20 K) measured again the photoemission in this energy range: they confirmed by means of a controlled surface contamination of the sample that the 3 eV structure has a partial surface character, as suggested in earlier studies [5, 6]. In these works the sample surfaces were prepared by ionic bombardment followed by annealing. However, it is well known that this treatment tends to induce a surface roughness, leading to a non-conservation of $k_\parallel$ for photoelectrons traversing the surface barrier, and that the consequent change $\Delta k_\parallel$ then integrates the photoemission signal in k space for some values of the polar angle [5, 6]. In our work, instead, both sample surfaces have been cleaved *in situ* and measurements have been made for two positions of the plane of analysis giving complementary and reliable information. In figure 2, we see that the maximum energy displacement of the peak C 4 eV occurs close to $\theta \approx 33^\circ$, while its energy position is close to $E_B \approx 3$ eV, near $\theta = 0^\circ$ and 60°. The energy position of this peak is plotted versus the $k_\parallel$ wavevector in figure 4 (squares and points): the experimental curve has a symmetrical minimum (at 4 eV) for $k_\parallel \cong 0.8$ Å^{-1}, and then disperses towards 3 eV for $k_\parallel = 0$ and 1.6 Å^{-1}. Now, if one considers that the direction $\bar{\Gamma}\bar{M}\bar{\Gamma}$ of the SBZ is intercepted for this position of the plane of analysis, one sees that the band minimum

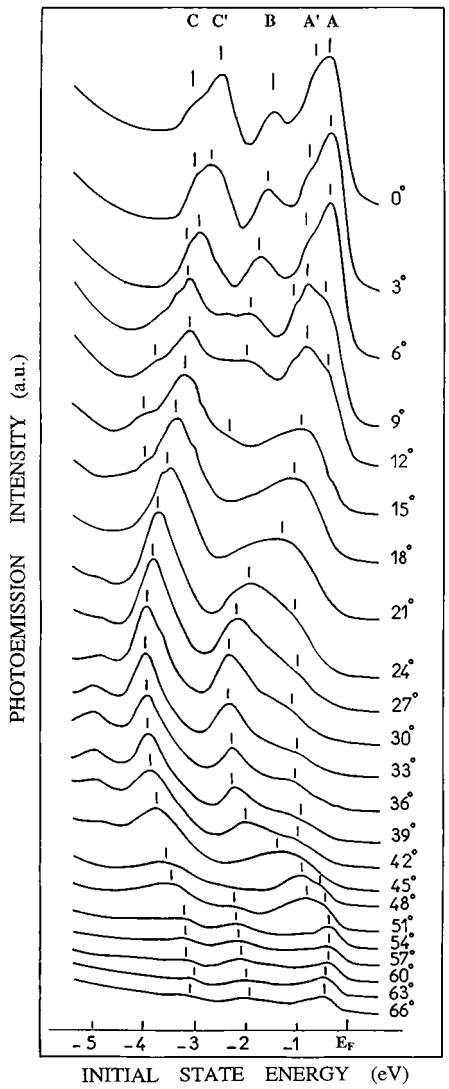

Figure 2. Angle resolved NeI photoemission spectra in the ΓLX plane of the Brillouin zone.

matches well the $\bar{M}$ point position at the zone border, and that, in addition, both end points of the $k_\parallel$ axis correspond to the $\bar{\Gamma}$ point at the zone centre of the repeated BZ. In figure 3, a similar behaviour is observed for the distribution curve of the peak C, measured in the orthogonal plane of analysis; that is, starting from the value of the polar angle $\theta = 0^\circ$, which is common to the two planes of analysis (φ and $\varphi + \pi/2$), one sees that the same evolution characterizes the photoemission behaviour of the peak C. In figure 5, we see that its dispersion curve reaches the band minimum for $k_\parallel = 0.9$ Å^{-1} (at 4.1 eV), and that for larger values of $k_\parallel$ the band approaches the symmetry point near $k_\parallel = 1.4$ Å^{-1} (at about 3.6 eV). In this plane of analysis we can sample the symmetry line $\bar{\Gamma}\bar{K}\bar{X}$ in the SBZ: as a matter of fact, the energy positions of the observed singularities fit well the positions of the critical points $\bar{K}$ and $\bar{X}$ (0.92 Å^{-1} and 1.38 Å^{-1}). Thus, the angle resolved photoemission data measured

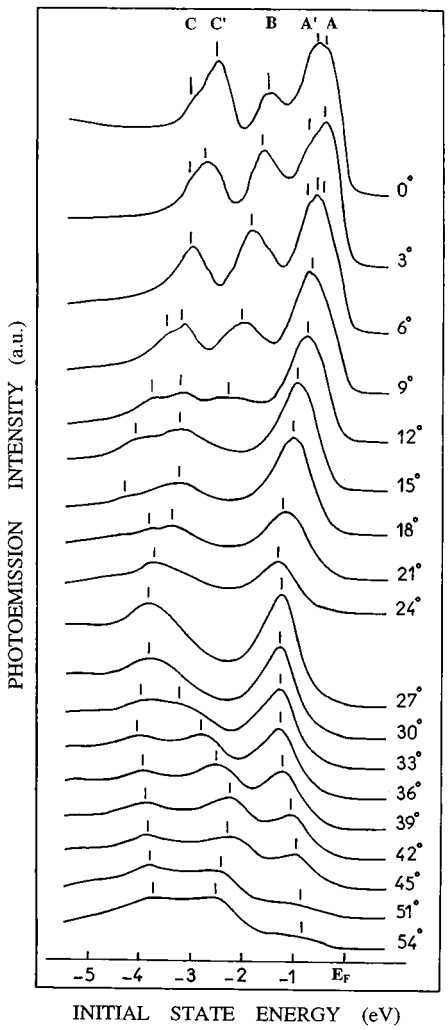

Figure 3. Angle resolved NeI photoemission spectra in the ΓWK plane of the Brillouin zone.

for the structure C in the two planes of analysis are well described along the symmetry lines indicated. We see in figures 4 and 5 that at the critical points $\bar{\Gamma}$, $\bar{M}$, $\bar{K}$ and $\bar{X}$ the dispersions of the electronic states are strongly affected by the curve singularities (extremum or saddle points). We note, in addition, that the symmetrical behaviour of the dispersion curve around the point $\bar{M}$ is required by the crystal periodicity and is often used as a cross-check for band dispersions of complicated systems. We also see that, going beyond the $\bar{M}$ point, the observed SS peak reverses its dispersion and traces its way back to the $\bar{\Gamma}$ point of the second hexagonal SBZ. One typical example of this behaviour is shown by the two-dimensional energy bands in graphite [18, 19]. Thus, the C band, whose energy position is essentially independent of the photon energy in normal photoemission and is not very sensitive to surface contamination (see figure 2 of [5]), is now strongly dispersing with the wavevector component $k_{\|}$ parallel to the sample surface, according to the symmetry of the SBZ. These facts allow us to conclude that

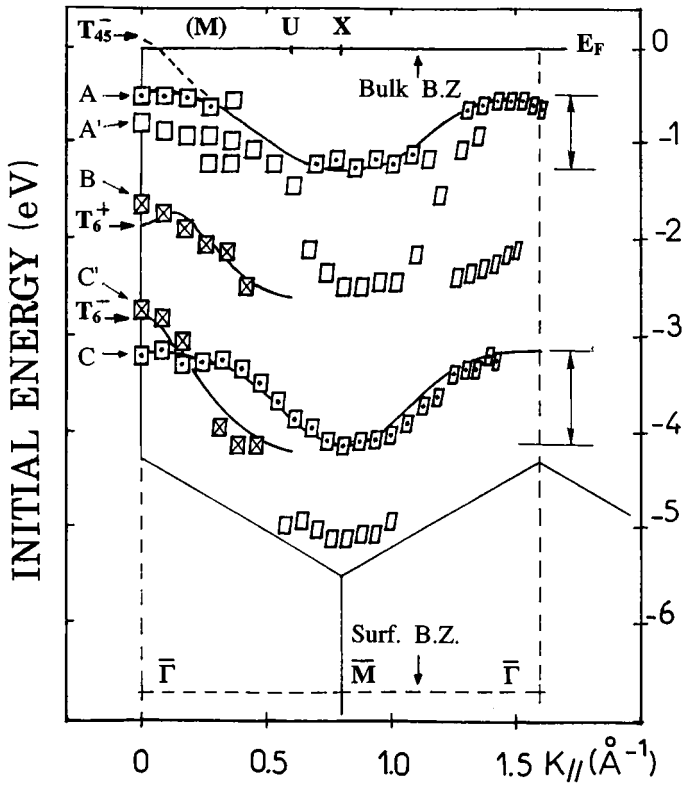

Figure 4. Experimental structure plot of the initial state energy $E(k_\parallel)$ for Bi(111)/ΓLX and cut through the surface Brillouin zone in the repeated scheme, showing the $\bar{\Gamma}\bar{M}\bar{\Gamma}$ symmetry line. The experimental points (squares and crosses) indicate the bulk band dispersions: comparison with theory (Golin [10]) along the symmetry line TMU is shown. The experimental points (squares and points) indicate the surface band dispersions.

this structure can be assigned to surface state emission, although it might have an important contribution from bulk (surface resonance), as was remarked in earlier studies [5, 7]. In fact, close to the peak C (in figure 2) we observe an electronic structure (peak C′), dispersing near 4 eV for θ between 9° and 18°. In figure 4, we have then connected these experimental points to the C′ peak (squares and crosses) measured in normal photoemission ($\theta = 0°$) at low photon energy. This structure thus corresponds to the C′ peak dispersing in normal photoemission at low energy, when the photon energy varies between 17 and 28 eV. Its initial state energy $E(k_\parallel)$ then shows a dispersion qualitatively similar to that of the valence band T_6^--U calculated by Golin. However, in order to obtain a better agreement with the experimental data, we had to shift down the Golin valence band by 0.75 eV. In figures 3 and 5, the structure C′, obtained for the other position of the plane of analysis, is also in qualitative agreement with Golin's valence band T_6^--W and again the agreement with the experiment is improved, if the same downward energy shift (0.75 eV) is made. The dispersion of the C′ peak, along the TU and TW lines, is also consistent, in terms of band picture description, with the valence band plots along the ΓT line obtained in normal photoemission [6], which has shown that the T point is reached for photon energy of about 17 eV. In figure 2, one also notes a weak structure slightly dispersing between 4.5 and 5 eV (for θ values between 30° and 45°). Its plot is symmetrical around the

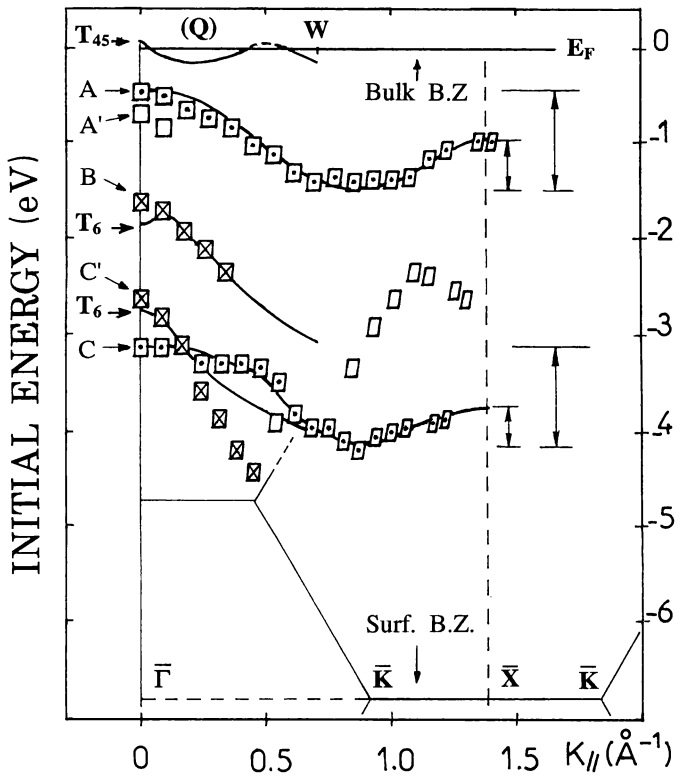

Figure 5. Experimental structure plot of the initial state energy $E(k_{\|})$ for Bi(111)/ΓWK and cut through the surface Brillouin zone in the repeated scheme, showing the $\bar{\Gamma}\bar{K}\bar{X}$ symmetry line. The experimental points (squares and crosses) indicate the bulk band dispersions: comparison with theory (Golin [10]) along the symmetry line TQW is shown. The experimental points (squares and points) indicate the surface band dispersions.

X point and seems to agree reasonably with Golin's band structure along the USX symmetry line (see figures 1 and 4): we tentatively assign this feature to a DOS effect near the point X of the BZ. We have found that the total width of the p bands is about 5 eV, close to the 4 eV value calculated by Golin [10].

Let us now consider the feature B observed around $E_B = 2$ eV in figure 2: this structure disperses between 2 and 3 eV, when the polar angle varies between 0° and 15°. The experimental points, when reported in the plane $(E, k_{\|})$, form a curve whose energy position and trend are very close to that of Golin's valence band T_6^+-U (figure 4). We find again a good qualitative agreement between the experimental data and the predictions of the empirical pseudopotential model (EPM), although in order to fit the theoretical curves to experimental points it is necessary to lower the calculated valence band T_6^+-U by 0.2 eV, on average. The same attribution and energy shift (0.2 eV) are also consistent with the experimental results obtained on the other plane of analysis (figures 3 and 5). The worse energy definition of feature B in the two symmetry directions investigated (for θ larger than 15°) can be understood if one considers that the electron wavevector enters the next BZ along a line of lower symmetry. In figure 3, we also note the presence of a strong dispersing structure between 2 and 4 eV, for θ between 27° and 54°: this feature, which seems of difficult interpretation at the moment,

is probably related to an *umklapp* process (see the points plotted between 0.8 and 1.3 Å^{-1} in figure 5). A process of this kind was, for example, considered in Cu(110) along the ΓKX line in order to plot some experimental points belonging to the Σ_4 band [20]. In addition, a new peak occurs in the same energy range in figure 2. The position of this peak remains almost constant in the vicinity of 2.3 eV for θ between 24° and 39°. We observe a qualitative agreement between this peak and the Golin band in the vicinity of the L_S critical point. Here again, it is likely that the mapping of this structure (near L_S) might be the result of a DOS effect (see figure 2 of [10]).

Finally, between the Fermi level and 1.5 eV binding energy, we observe a broad and complex structure (A and A′) for the two positions of the plane of analysis (see figures 2 and 3). This energy region near E_F was earlier studied by Jezequel *et al* [5] and Patthey *et al* [7] along the $\bar{\Gamma}\bar{K}$ line of the SBZ. The excellent quality of the latter measurements has confirmed the existence of a SS near E_F in the spin–orbit open gap between the two bulk derived structures. The feature A presents in the ΓWK plane (figure 3) a simple profile: when we report the experimental points in the plane (E, $k_\parallel$) of figure 5, we see that the behaviour of this band is consistent with the symmetry of the SBZ. The extremum points are coincident with the critical points of the Brillouin zone, and the trend is similar to that of the surface state C discussed earlier. Patthey's results show that the complex profile of the band A in this energy range is well resolved, exhibiting three peaks in normal photoemission, and that the central peak corresponds to the surface state band in the spin–orbit gap. In figure 2, the band A in the plane ΓLX presents again a complex profile, having, besides the main structure, some faint shoulders accompanying the main peak. When this band is plotted in k space, we see that the energy dispersion of the main peak A roughly follows the symmetry of the SBZ along the direction $\bar{\Gamma}\bar{M}\bar{\Gamma}$ (figure 4). The weak feature A′ close to the surface state A is found in an energy range where Golin's calculation indicates the presence of the bulk valence band T_{45}^{-}-U (dashed line in figure 4). It is thus likely that the feature A′ (practically absent in the plane of analysis TWK) might be partly due to this bulk electronic band.

The less good experimental resolution which affects our data compared to Patthey's spectra is only detrimental to our results near the Fermi energy, because of the large hole lifetime in this energy range. At higher binding energy, however, where the hole lifetime is somewhat shorter, our experimental resolution is good enough to follow the band dispersions. Moreover, the thermally induced peak broadening and intensity reduction (a minor effect) mostly affect the peaks close to the Fermi energy and, in particular, the surface peak observed in the spin–orbit gap at the Bi(111) surface.

4. Conclusions

By means of a new angular resolved ultraviolet photoelectron spectroscopy study of the single crystal Bi(111) face we have sampled the intrinsic surface states in the surface Brillouin zone. We have confirmed the surface character of the non-dispersing electronic states measured along the ΓT line in normal photoemission. The present measurements show that photoemission from the cleaved (111) face of Bi is mainly due to surface state features occurring together with bulk valence bands. Within the limits of the approximations considered in our study, we have also mapped bulk valence bands along the TMU and TQW symmetry lines of the Brillouin zone and compared them to Golin's band structure calculation which reproduces the experimental p-like band dispersions correctly between E_F and 5 eV, although an energy shift (by about 0.20 eV and 0.75 eV) of the theoretical p-like bands along the symmetry lines TMU and TQW is needed to better agree with the experimental data.

Note added in proof. An ARUPS study of the valence band electronic structure of the semimetal Bi(111) by Tanaka A *et al* 1999 *Phys. Rev.* B **59** 1786–91 has been recently pointed out to us. We note that their experimental energy dispersions in the photoelectron detection plane Γ-L-X match, in general, rather well our structure plot in figure 4, and, moreover, that their conclusions are similar to ours in regards to the EPM calculation, which fails to reproduce the experimental results quantitatively.

References

[1] Himpsel F J 1983 *Adv. Phys.* **32** 1–51 and references therein
[2] Desjonquères M C and Spanjaard D 1993 *Concepts in Surface Physics* (Berlin: Springer)
[3] Hansson G V and Flodstrom S A 1978 *Phys. Rev.* B **18** 1572
Hansson G V and Flodstrom S A 1978 *Phys. Rev.* B **18** 1562
[4] Levinson H J, Greuter F and Plummer W E 1983 *Phys. Rev.* B **27** 727
[5] Jezequel G, Petroff Y, Pinchaux R and Yndurain F 1986 *Phys. Rev.* **33** 4352
[6] Jezequel G, Thomas J and Pollini I 1997 *Phys. Rev.* B **56** 6620 and references therein
[7] Patthey F, Schneider W D and Micklitz H 1994 *Phys. Rev.* B **49** 11 293
[8] Weitzel B and Micklitz H 1991 *Phys. Rev. Lett.* **66** 385
[9] Ley L, Pollack R A, Kowalczyk S P, McFeely R and Shirley D A 1973 *Phys. Rev.* B **8** 641
[10] Golin S 1968 *Phys. Rev.* **166** 943
[11] Norris C and Wotherspoon J T 1976 *J. Phys. F: Met. Phys.* **6** L263
[12] Baer Y and Myers H P 1977 *Solid State Commun.* **21** 833
[13] Pendry J B and Gurman S J 1975 *Surf. Sci.* **49** 87
[14] Feder R and Sturm K 1975 *Phys. Rev.* B **12** 537
[15] Kevan S D, Stoffel N G and Smith N V 1985 *Phys. Rev.* B **32** 4956
[16] Anishchik V, Falicov L M and Yndurain F 1976 *Surf. Sci.* **57** 375
[17] Thomas J and Pollini I 1999 *Rev. Sci. Instrum.* submitted
[18] Williams P M 1977 *Nuovo Cimento* B **38** 216
[19] McGovern I T, Eberhart W, Plummer E W and Fischer J E 1980 *Physica* B **99** 415
[20] Thiry P, Chanderis D, Lecante J, Guillot C, Pinchaux R and Petroff Y 1979 *Phys. Rev. Lett.* **43** 82